

## PAPER

View Article Online  
View Journal | View Issue



Cite this: *Environ. Sci.: Processes  
Impacts*, 2023, 25, 850

# Arsenic in Lake Geneva (Switzerland, France): long term monitoring, and redox and methylation speciation in an As unpolluted, oligo-mesotrophic lake†

Montserrat Filella,<sup>a</sup> Sebastian Wey,<sup>a</sup> Tomáš Matoušek,<sup>b</sup> Mathieu Coster,<sup>c</sup>  
Juan-Carlos Rodríguez-Murillo<sup>d</sup> and Jean-Luc Loizeau<sup>a</sup>

Arsenic speciation was followed monthly along the spring productivity period (January–June 2021) in the Petit Lac (76 m deep) and in April and June 2021 in the Grand Lac (309.7 m deep) of Lake Geneva (Switzerland/France). Lake Geneva is presently an oligo-mesotrophic lake, and As-unpolluted. The water column never becomes anoxic but the oxygen saturation at the bottom of the Grand Lac is now below 30% owing to lack of water column mixing since 2012. Thus, this lake offers excellent conditions to study As behaviour in an unpolluted, oxidic freshwater body. The following ‘dissolved’ As species:  $iAs(III)$ ,  $iAs(III + V)$ ,  $MA(III)$ ,  $MA(III + V)$ ,  $DMA(III + V)$ , and TMAO were analysed by HG-CT-ICP-MS/MS. Water column measurements were complemented with occasional sampling in the main rivers feeding the lake and in the interstitial waters of a sediment core. The presence of  $MA(III)$  and TMAO and the predominance of  $iAs(V)$  in lake and river samples has been confirmed as well as the key role of algae in the formation of organic species. While the total ‘dissolved’ As concentrations showed nearly vertical profiles in the Petit Lac, As concentrations steadily increase at deeper depths in the Grand Lac due to the lack of mixing and build up in bottom waters. The evaluation of 25 years of monthly data of ‘dissolved’ As concentrations showed no significant temporal trends between 1997 and 2021. The observed seasonal character of the ‘dissolved’ As along this period coincides with a lack of seasonality in As mass inventories, pointing to a seasonal internal cycling of As species in the water column with exchanges between the ‘dissolved’ and ‘particulate’ (i.e., algae) fractions.

Received 23rd October 2022  
Accepted 1st February 2023

DOI: 10.1039/d2em00431c

rsc.li/espi

## Environmental significance

The presence and fate of arsenic in aquatic environments have been widely studied, but its chemical speciation and cycling in lakes have received relatively little attention so far. Moreover, most of the lakes studied were shallow, eutrophic, and heavily polluted with arsenic. The present study investigates the behaviour of arsenic in a natural environment at background concentrations, thus providing a basis to better assess the fate of this element in polluted environments. To this end, we carefully applied state-of-the-art analytical techniques to the waters of a deep, oligo-mesotrophic, arsenic unpolluted lake that never becomes anoxic. Collected data on the speciation of arsenic each month during the spring productivity period show that the production and presence of reduced and methylated As species are mainly biota related. In addition, the availability of 25 years of monthly data on arsenic concentrations in this lake allows us to contextualize our findings and provides additional insight into the behaviour of arsenic.

## Introduction

Arsenic (As) is among the trace elements receiving the most public and scientific attention mainly because of its occurrence in contaminated groundwater and association with human health problems. Even though the toxicity of As has been known for a long time,<sup>1</sup> the massive pollution of drinking water by As in Bangladesh, where as many as 35–50 million people were exposed to toxic levels,<sup>2,3</sup> put As pollution on the environmental agenda. Moreover, the problem is not restricted to Bangladesh but is widespread across the planet.<sup>4</sup>

<sup>a</sup>Department F.-A. Forel for Environmental and Aquatic Sciences, University of Geneva, Boulevard Carl-Vogt 66, CH-1205 Geneva, Switzerland. E-mail: montserrat.filella@unige.ch; Sebastian.Wey@etu.unige.ch; jean-luc.loizeau@unige.ch

<sup>b</sup>Institute of Analytical Chemistry of the Czech Academy of Sciences, Veveří 97, 602 00 Brno, Czech Republic. E-mail: matousek@biomed.cas.cz

<sup>c</sup>Service de l'écologie de l'Eau, Geneva, Switzerland. E-mail: mathieu.coster@etat.ge.ch

<sup>d</sup>Museo Nacional de Ciencias Naturales, CSIC, Serrano 115 dpdo, E-28006 Madrid, Spain. E-mail: jcmurillo@mncn.csic.es

† Electronic supplementary information (ESI) available. See DOI: <https://doi.org/10.1039/d2em00431c>



of aspects such as sampling frequency and the meaning and quality of analytical data used on the results obtained, we have mainly focused on two aspects: (i) tracking As speciation along the spring productivity period in an oligo-mesotrophic, As-unpolluted lake, and (ii) analyzing the temporal trends of As concentrations in the lake thanks to the existence of 25 years of monthly data of ‘dissolved’ As concentrations – rather uncommon information.

## Materials and methods

## Study site

Lake Geneva has a monomictic regime with infrequent complete overturns in recent decades. After the last entire mixing of the water column in 2012, mixing in the Grand Lac has been limited to the upper layer ( $\sim 130\text{--}150$  m depth), preventing oxygen from reaching the lake bottom through mixing, *i.e.*, oxygen concentrations at the bottom never exceeded  $4\text{ mg L}^{-1}$  during the entire year after 2016 and sediments remained poorly oxygenated.<sup>29</sup> The Petit Lac mixes entirely once a year, and the build up of anoxia has never been observed.

Lake Geneva undergoes regular physicochemical, biological and micropollutant monitoring. Samples across the water column are taken once a month in the Petit Lac at sampling site GE3 (6.2197° E/46.2994° N) by the Service de l'Écologie de l'Eau of the Canton of Geneva (SECOE), Switzerland. Similar analyses are conducted at least once a month at the sampling location SHL2 (6.5887° E/46.4527° N), which corresponds to the deepest point of the lake.<sup>29</sup>

The phytoplankton community in Lake Geneva shows a seasonal pattern.<sup>30</sup> In early spring, a first phytoplankton bloom is followed by an increasing zooplankton community that exerts heavy grazing pressure on the phytoplankton. This pattern leads to a clear water phase which usually occurs in June. However, global warming seems to make this phenomenon appear earlier and, in recent years, the clear water phase has been observed earlier in the season.<sup>30</sup>

Lake Geneva is fed by more than 60 rivers and streams. All tributaries longer than 10 km are listed in Table SI3.† Most incoming water (73%) enters the lake *via* the River Rhone to the east. The Rhone River has a glacial-nival regime with high flows in late spring and summer; water discharge values for the period 1935–2019 and for 2021 are shown in Fig. SI1.† Four other tributaries were sampled (Aubonne, Dranse, Venoge, and



Table 1 Published As speciation studies in lakes

Lake	Lake depth/ m	Characteristics	Water sampled	# Sampling campaigns	Filtration	Technique	Inorganic species	Organic species	Ref.
Pavin, France	90	Permanently stratified	Profile	1: Dec	0.4 µm	HG-AAS	iAs(III) and iAs(V)	—	15
9 lakes, US	20	Seasonally anoxic	Surface	1	0.4 µm	HG-AAS	iAs(III) and iAs(V)	MA and DMA	16
Davis Creek Reservoir, US			Profile	5: Jul, Sep, Oct, Dec, and Feb					
Greifen, Switzerland	Max: 17.7	Seasonally anoxic	Profile	Monthly: Aug 89 to Jan 91	0.45 µm	HG-AAS	iAs(III) and iAs(V)	MA(III + V) and DMA(III + V) <sup>a</sup>	17
Aberjona watershed		Strongly As polluted	Surface	1 (5 locations)	0.45 µm	HG-AAS	iAs(III) and iAs(V)	MA(III + V) and DMA(III + V)	18
Hall's Brook	Average: 3	Eutrophic	Profile	11: Fall-spring					
Upper Mystic	~20	Eutrophic	Profile	6: Fall-spring	0.45 µm	HG-AAS	iAs(III) and iAs(V)	DMA(V) mentioned	19
Lower Mystic	~20	Historically polluted	Profile	Several (unclear when)	Not mentioned	HG-AAS	iAs(III) and iAs(V)	MA, DMA, TMAO, and	20
Upper Mystic, US	25	Strongly As polluted	Surface	1				M <sub>n</sub> As <sup>III</sup> (SR) <sub>3-n</sub> (n = 1, 2, 3)	
Meg, Keg and Peg, Canada	Max: < 2							MA(III), MA(V), DMA(III), and DMA(V)	21
Biwa, Japan; dredged area South basin	ca. 12		Profile	Feb–Oct 1993 and apr–Dec 1994	0.45 µm	HG-AAS	iAs(III) and iAs(V)	MA(III + V), MA(III), DMA(III + V), and DMA(III)	22
Biwa, Japan	Average: 44	Mesotrophic, eutrophic	Profile	Monthly: 2 years	0.45 µm	HG-AAS	iAs(III) and iAs(V)	MA and DMA <sup>b</sup>	23
18 lakes, Japan	Mostly shallow, median: 4.1	Eutrophic	Surface	2: Summer & winter	0.45 µm	HG-AAS	iAs(III) and iAs(V)		
Mohawk, US	1–7	As polluted	Profile	2: Sep & Oct	0.45 µm	Not mentioned	iAs(III) and iAs(V)	MA and DMA	24
Tailhu, China	Average: 2	From hypereutrophic to mesotrophic	Surface	4: Autumn, summer, winter, and spring	0.45 µm	HPLC-ICP-MS	iAs(III) and iAs(V)	MA(V) and DMA(V)	25
4 small subarctic lakes, Canada	0.8–6.9	As polluted, ice-covered	Surface	Several, covering 2 open water and 2 ice covered seasons	0.45 µm	HG-AAS	iAs(III) and iAs(V)	—	26
Yamdruk, Tibet	Median: 30, max: 60	As polluted, cold lake	Surface	2: dry & wet seasons	0.45 µm	HPLC-HG-AFS	iAs(III) and iAs(V)	DMA (only in one sample)	27
Aha reservoir, China	Average: 13		Surface	4 seasons	0.45 µm	HPLC-ICP-MS	iAs(III) and iAs(V)	MA and DMA	28

<sup>a</sup> The majority of the samples were only analysed for iAs(III) and iAs(V). <sup>b</sup> Species called UV-As(III + V), UV-MA, UV-DMA were also measured.

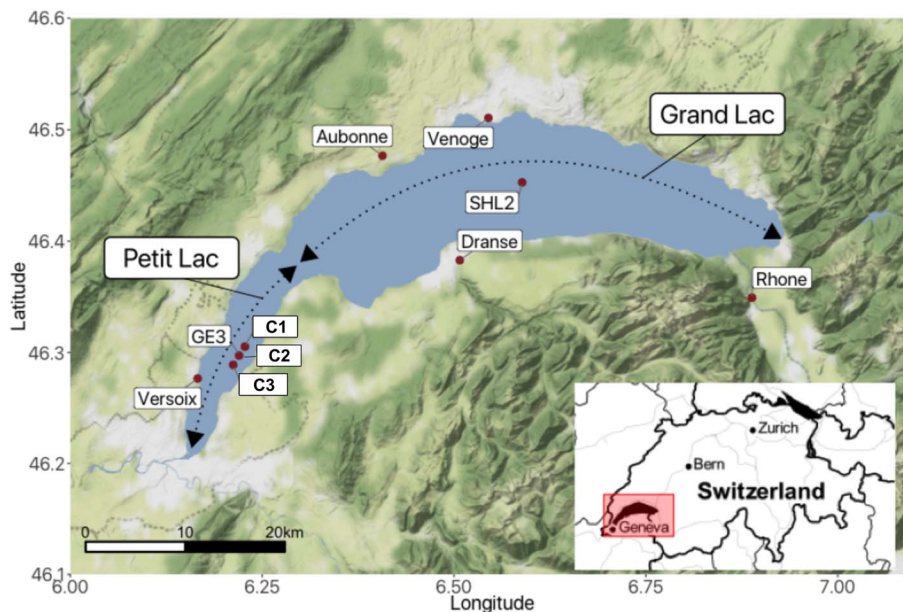


Fig. 1 Lake Geneva (Switzerland/France) with sampling locations for rivers, lake and sediments.

Versoix) in this study. Their regimes are pluvial with the highest discharge observed during winter and spring.

### Sampling

**Lake water.** Sampling sites are shown in Fig. 1. Water samples through the water column were collected monthly (intervals of 21–35 days) between January and June 2021 at sampling site GE3. Water samples were taken at ten depths (0, 2.5, 5, 7.5, 10, 15, 20, 30, 50, and 65 m). At SHL2, samples were taken on 20 April and 14 June 2021 at 13 different depths (0, 5, 10, 15, 20, 25, 30, 35, 50, 100, 150, 200, and 300 m).

Lake water samples were collected with Niskin bottles. Lake water samples at GE3 were transferred into 125 mL HDPE flasks (Nalgene) and stored refrigerated until further treatment. The flasks were cleaned with acid (1%  $\text{HNO}_3$ ) for at least one day, followed by incubation with Milli-Q water for at least another day. The flasks were further rinsed with lake water from the corresponding depth before water sampling. Lake water samples at SHL2 were transferred from the Niskin bottle into a glass beaker and immediately treated on site. In both cases, 15 mL was filtered using polyethersulfone (PES) filters of pore-size 0.20  $\mu\text{m}$  and single-use syringes (HSW Henke-Ject). The samples were transferred into trace metal free centrifuge tubes (VWR) and 150  $\mu\text{L}$  0.2 M EDTA solution was added per 15 mL sample. The samples were refrigerated with cooling elements during the transfer from Geneva to Prague, where speciation analysis was carried out, and stored at 4  $^\circ\text{C}$  after arrival. Analyses for TMAO,  $\text{MA(III)}$  and  $\text{iAs(III)}$  were performed within 2–10 days from sampling. Analyses for  $\text{iAs(III + V)}$ ,  $\text{MA(III + V)}$  and  $\text{DMA(III + V)}$  were carried out within 3–13 days from sampling. Tests on preservation and matrix effects were performed in January 2021, before the first lake sampling campaign. The preservation of filtered samples (0.20  $\mu\text{m}$ ) stabilized by 2 mM EDTA and stored at 4  $^\circ\text{C}$  was verified by repeated analyses.

**River water.** Five tributaries (Rhone, Venoge, Aubonne, Versoix, and Dranse) were sampled from 15–16 April and 22–23 June 2021. Location of the sampling points is given in Fig. 1 and coordinates are given in Table S14.† River water samples were drawn using typical household buckets and treated in the same manner as lake water samples immediately after collection.

**Sediment pore water.** Surface sediment cores were taken on 12 July 2021 at sampling locations C1 (6.2276° E/46.3052° N), C2 (6.2201° E/46.2971° N) and C3 (6.2123° E/46.2888° N), all at water depths higher than 65 m (Fig. 1). Sediment cores were taken with a gravity Uwitec-corer (Uwitec, Austria). Holes were drilled in the PVC coring tubes at distances of 1.5 cm prior to sampling. Subsequent pore water extraction was carried out using a Rhizon core solution sampler 5 cm with a membrane pore size of 0.12–0.18  $\mu\text{m}$  from Rhizosphere Research Products (Fig. S12†). Pore water samples were taken at approximately 1, 4, and 7 cm sediment depth. The surface sediment sample was of brownish colour, and it can be assumed that it was oxygenated. The pore water sample at 7 cm depth was taken from the core where the sediment was coloured black, suggesting reducing conditions. An additional water sample was taken directly above the sediment–water interface (supernatant). After extraction, 3 mL of pore water followed the treatment described above.

Previous sedimentological studies showed that surface sediments at this location consist mainly of silts, with 45% carbonates and 9% organic matter.<sup>31</sup>

### Analysis

**Total ‘dissolved’ arsenic.** Total ‘dissolved’ As concentrations ( $\text{As}_{\text{tot,dis}}$ ) were measured in all samples by inductively coupled plasma mass spectrometry (ICP-MS). Analyses of  $\text{As}_{\text{tot,dis}}$  at sampling site GE3 were carried out as part of the lake monitoring by the SECOE with an ICP-MS Agilent 7900 in high energy He mode. The samples taken in June 2021 at SHL2 and during





the second river sampling campaign were analysed at the Institute of Analytical Chemistry of the Czech Academy of Sciences, Prague, with an ICP-MS/MS Agilent 8900 in O<sub>2</sub>-mode (+16 mass shift). River samples collected in April 2021 and all samples from the sampling campaign at SHL2 on 20 April 2021 were analysed at EPFL, Lausanne (ICP-MS/MS Agilent 8900).

Concentrations of As<sub>tot,dis</sub> are available at site GE3 from 1997 and are used in this study to evaluate temporal trends. The concentrations were measured by ICP-MS on a Fisons PQ2+ before 2006, on a Thermo-Fisher X7 II from 2006 to 2015, and with an ICP-MS Agilent 7900 in high energy He mode since 2015 at SECOE. The analytical accuracy was followed by analysing the certified reference materials (CRM) SLRS-4, SLRS-5 and SLRS-6 (National Research Council Canada). The analytical laboratory is accredited for the analysis of the trace elements in freshwaters (accreditation number: STS245; ISO norm 17 025).

**Arsenic speciation.** For full details of the analytical method description and validation see Section SI1†. Analysis of inorganic and methylated As species was conducted following the method described in Matoušek *et al.* (2013),<sup>32</sup> García-Figueroa *et al.* (2021)<sup>33</sup> and Filella and Matoušek (2022)<sup>34</sup> by hydride generation (HG) followed by cryotrapping (CT) in a U-tube under liquid nitrogen. Detection was performed by ICP-MS/MS. The analysed species were iAs(III), iAs(III + V), MA(III), MA(III + V), DMA(III + V) and TMAO. The methylated species were identified based on the production of different methyl substituted hydrides upon HG and their collection and separation in a cryotrap where generated arsanes are collected and then released sequentially according to their boiling points. The determination of the oxidation state of individual species was based on the selective generation of trivalent species at pH 6. iAs(III), MA(III) and TMAO were determined from one aliquot while the analysis of a second one, pre-reduced with L-cysteine, gave iAs(III + V), MA(III + V), and DMA(III + V).<sup>35</sup> The complete HG-CT-ICP MS/MS parameters are shown in Table SI5†.

For each series of As speciation analysis, a certified river water sample (SLRS-6) from the National Research Council of Canada was included as a quality control.

## Other data

Monthly ancillary data (*e.g.*, temperature, pH, conductivity, concentrations of oxygen, nutrients, and various metals, and phytoplankton counting) for location GE3 were provided by SECOE. They cover the period January 1997–December 2021. The analytical instruments used for metal analyses were changed twice since 1997. Analyses were performed by ICP-MS on a Fisons PQ2+ before 2006 and on a Thermo-Fisher X7 II from 2006 to 2015. Since 2015, concentrations are measured on an Agilent 7900. Ancillary data for sampling location SHL2 and ancillary data for sampling location SHL2 were provided by CARTEL (Alpine Center for research on trophic networks and limnic ecosystems), France.

## Time series data statistical treatment

Non-parametric methods are required to analyse temporal trends of trace element concentrations in water because data do

not typically follow a normal distribution.<sup>36</sup> Thus, temporal trends can be studied by applying Mann–Kendall (MK) or seasonal Mann–Kendall (SMK) methods,<sup>37,38</sup> depending on the presence or absence of seasonality in the data. The statistical significance of the trends is obtained in MK methods by applying the Z-statistic test of the sum of signs of the differences between every pair of values; Z shows a normal distribution, and therefore, the statistical significance of the temporal trend can be evaluated by using the *p* value. The Kruskal–Wallis test of equal medians for the data classified by depth and month is used to test for seasonality.

Fourier power spectra of concentration time series have also been calculated to confirm seasonality. The REDFIT method used fits a first-order autoregressive process (AR(1)) to the concentration time series to calculate the Fourier spectrum.<sup>39</sup> The 95% confidence limit of that spectrum is obtained with a Monte Carlo calculation. Spectral peaks above that confidence limit are considered as statistically significant.

Calculation programs used for MK and SMK tests are from <https://www.mathworks.com/matlabcentral/fileexchange/11190-mann-kendalltau-b-with-sensmethod-enhanced/content/ktaub.m> adapted by us. Kruskal–Wallis tests and REDFIT were performed with PAST.<sup>40</sup>

# Results and discussion

## Questions related to analytical methods

**Quality issues in the analysis of arsenic species.** Under the experimental conditions used, method LODs were assessed to be 0.9 and 1.2 ng L<sup>-1</sup> for iAs(III) and iAs(III + V), respectively, 0.1 ng L<sup>-1</sup> for monomethyl species and TMAO and 0.2 ng L<sup>-1</sup> for DMA(III + V). Values for all species were above the LOD in all analysed samples, with the exception of MA(III) data in January and February GE3 profiles. The uncertainty of the species concentration data was better than 4% relative standard deviation (RSD) except for TMAO with 11% RSD (see Section SI1 and Table SI6†).

Rigorous tests on species stability and sample conservation were performed prior to analysis. Filtered samples (0.20 µm) stabilized by 2 mM EDTA addition and storage at 4 °C was proven a suitable strategy for all species including iAs(III) redox stability at tens of ng L<sup>-1</sup> level for several months. This method was superior to acidification by HNO<sub>3</sub> to pH 1 mainly due to minor method specific issues related to redox speciation based on pH selectivity of HG (see Section SI1†).

Great care was taken to verify that the small iAs(III) concentration of few tens of ng L<sup>-1</sup> present in practically all samples was not due to an analytical artefact. However, no iAs(III) was observed in iAs(V) standards, nor in CRM SLRS-6 (acid conserved to pH 1.5). Additionally, less than 10 ng L<sup>-1</sup> was found in SHL2 profile samples at depths higher than 100 m. All these facts makes us believe that the presence of low iAs(III) concentrations is real.

Due to the limited selectivity of the pH selective HG step, 1% of 'apparent' MA(III) and 6% of 'apparent' DMA(III) were generated from pentavalent forms, and assessed from the slopes of MA(V) and DMA(V) calibrations without prereduction. In all



**Table 2** Concentrations of total dissolved arsenic ( $As_{tot,dis}$ ) and arsenic species in river samples. Sampling campaign April 2021. All concentrations in  $ng\ L^{-1}$ 

River	Date	Time	$As_{tot,dis}$	sumAs	iAs(v)	iAs(III)	MA(III + v)	DMA(III + v)	TMAO
Rhône	16 April	08:50	1190	1247	973	230	5.9	36.2	2.2
		09:50	1151	1139	868	225	5.2	38.6	2.4
		10:50	1200						
		11:50	1166						
		12:50	1204						
Aubonne	16 April	16:20	187	161	110	37.2	0.9	11.7	1.1
Dranse	15 April	09:00	134	116	62.2	42.7	0.9	9.3	0.5
Venoge	16 April	15:20	336	207	118	58.5	3.9	23.1	3.1
Versoix	16 April	17:20	219	158	106	25.7	1.6	23.0	1.4

analysed samples, the proportion of  $DMA(III)/DMA(III + v)$  observed corresponded to this ratio and  $DMA(III)$  is believed to be absent in the samples, probably because this species is extremely unstable and easy to oxidize.<sup>13,41</sup> On the other hand, a proportion of  $MA(III)/MA(III + v)$  higher than 1% and up to 10% was observed in samples except in January and February, sufficient to produce a distinctive profile. Caution should be, however, taken when interpreting  $MA(III)$  data, due to extremely low concentrations ( $2\ ng\ L^{-1}\ As$  or below) and potentially limited redox stability (see Section SI1†).

The sum of the concentrations of all investigated As species (sumAs), *i.e.* the sum of  $iAs(III + v)$ ,  $MA(III + v)$ ,  $DMA(III + v)$  and TMAO, in G3 was always lower by  $0.1\text{--}0.26\ \mu g\ L^{-1}\ As$  (*i.e.* 8–24%) than  $As_{tot,dis}$  (Tables SI7 and SI8†); a Kruskal–Wallis test performed on both sumAs and  $As_{tot,dis}$  shows that the assumption of equal means among several months can be refused ( $p$  value < 0.0001). SumAs and  $As_{tot,dis}$  however, closely followed the shape of the profiles along the season. Even an unexpected concentration drop in March 2021 was simultaneously observed in both, sumAs and  $As_{tot,dis}$ . Similarly, sumAs concentrations were always lower than  $As_{tot,dis}$  in the Grand Lac (Tables SI9 and SI10†). River samples showed the same behaviour (Tables 2 and 3) as those from the lake although differences seem to depend on the river with, for instance, values tending to agree more in the Rhône River than in other rivers.  $As_{tot,dis}$  and sumAs values agreed well in sediments (Table SI11†). Both the certified and the measured values of sumAs were lower in SLRS-6 (Table SI6†) than the

certified  $As_{tot,dis}$  of  $0.57 \pm 0.08\ \mu g\ L^{-1}$ , value recently confirmed by a value of  $0.58 \pm 0.04\ \mu g\ L^{-1}$ .<sup>42</sup> Three different laboratories contributed to the obtained values for  $As_{tot,dis}$  and the deviation from sumAs was similar. Discrepancies between  $As_{tot,dis}$  and sumAs had been attributed in the past to As organic compounds that are non-hydride reactive species,<sup>43–46</sup> but it is unclear how such species could uniformly be present in all samples and also explain our observations. This discrepancy has no practical consequence for the conclusions reached in this study.

**Quality issues in total ‘dissolved’ As concentrations: historical data.** Total ‘dissolved’ As concentrations ( $As_{tot,dis}$ ) for the period 1997 to 2021 are shown in Fig. 2. Three concentration zones can be observed that differ in precision and in the range of concentration values (*i.e.*, median values for each period are statistically different). Each concentration zone corresponds to one of the three ICP-MS instruments used during the years to measure trace element concentrations. The effect of the change of instruments on measured trace element concentrations has already been discussed for other chemical elements.<sup>47</sup> While improvement in precision is expected, the observed change in concentration median values remains difficult to explain. Some extent of positive error due to isobaric interferences cannot be excluded in older instruments, especially in the case of the pre-2006 instrument, a quadrupole ICP-MS without collision cell technology.

Arsenic concentrations in the second period (in red in Fig. 2) show a marked decrease around 2011. Plotting As values in

**Table 3** Concentrations of total dissolved arsenic ( $As_{tot,dis}$ ) and arsenic species in river samples. Sampling campaign June 2021. All concentrations in  $ng\ L^{-1}$ 

River	Date	Time	$As_{tot,dis}$	sumAs	iAs(v)	iAs(III)	MA(III + v)	DMA(III + v)	TMAO
Rhône	23 June	08:50	908	879	742	68.2	2.4	64.8	1.2
		09:50	767	752	668	58.6	1.6	22.4	1.2
		10:50	781	743	661	56.4	1.5	22.4	1.3
		11:50	721	713	625	52.3	1.5	24.5	1.2
		12:50	762	717	629	52.5	1.7	32.7	1.2
Aubonne	22 June	15:30	299	228	166	27.8	1.6	31.1	1.3
Dranse	22 June	19:00	269	212	121	22.8	2.1	64.9	0.9
Venoge	22 June	14:45	846	672	604	51.0	6.5	30.6	6.4
Versoix	22 June	12:50	295	240	181	33.4	2.5	20.3	2.5





**Fig. 2** (a) Monthly total 'dissolved' arsenic concentrations ( $As_{tot,dis}$ ) at all sampling depths at sampling site GE3 between 1997 and 2021. Different colours correspond to different analytical instruments (blue, period one; red, period two; green, period three; see text for details). (b) Same data with values of the CRM simultaneously measured ( $As_{tot} CRM_m$ ) and relative to their certified values ( $As_{tot} CRM_c$ ) (orange: SLRS-4, certified  $0.68 \pm 0.06 \mu g L^{-1} As$ ; turquoise: SLRS-5, certified  $0.413 \pm 0.039 \mu g L^{-1} As$ ). (c) Same data after normalisation by using the median concentration of each period.

CRMs measured at the same time as the samples and normalized to their certified value (Fig. 2b, SLRS-4 in orange, and SLRS-5 in turquoise) clearly shows that the observed decrease is due to an analytical artefact and is not caused by lake processes. Thus, period 2 will be excluded in further analysis of the data.

### Tracking arsenic along the spring productivity period

**Setting the context: physical characteristics of the water column during the spring productivity period.** From January to March, the Petit Lac was well-mixed and the temperature was constant across the depth (Fig. 3). The water column at



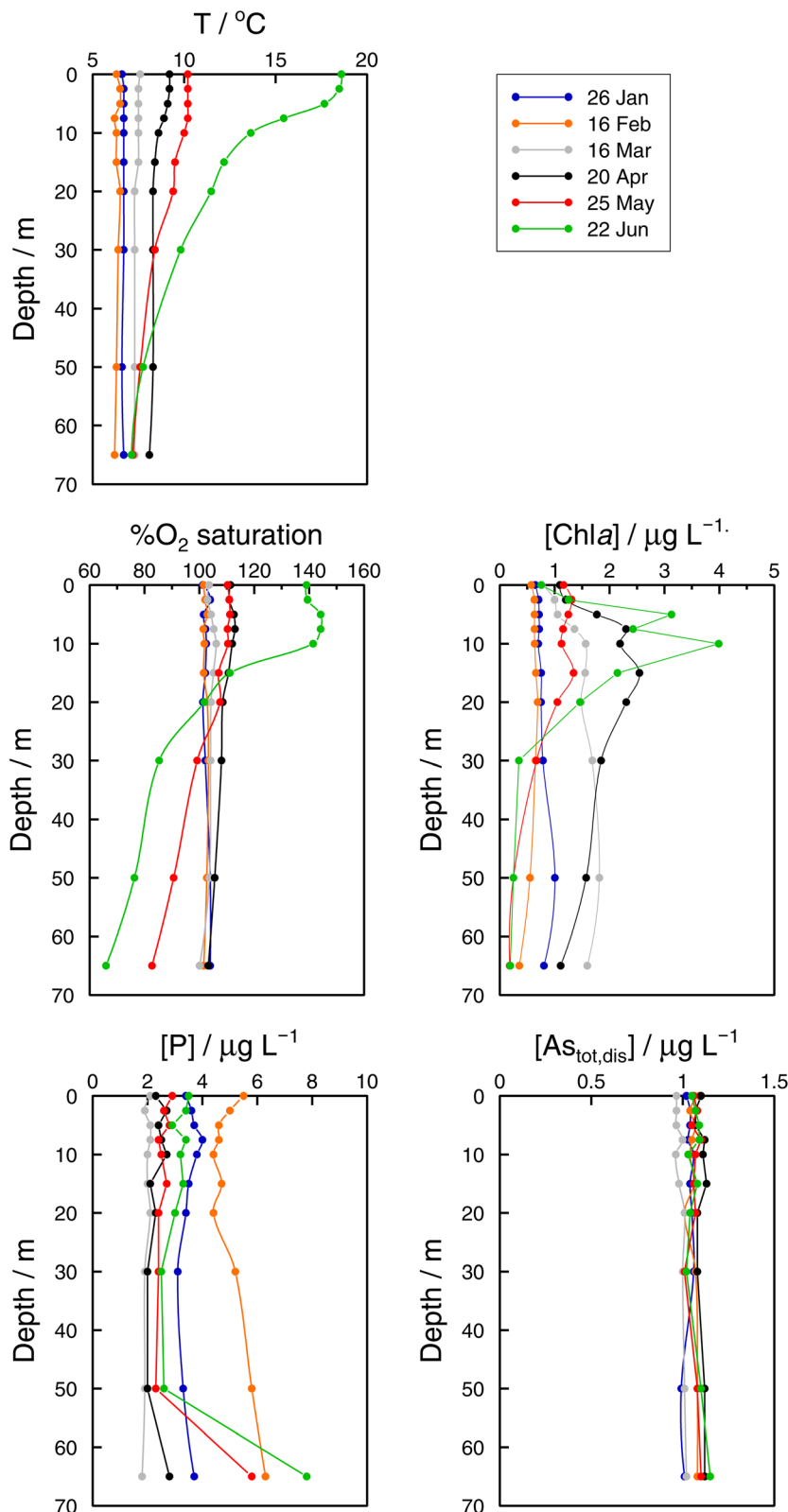


Fig. 3 Vertical profiles of temperature, percentage of  $O_2$  saturation, chlorophyll a, dissolved reactive phosphorus (DRP), and total 'dissolved' arsenic,  $As_{tot,disr}$ , concentrations in the Petit Lac (point GE3) from January to June 2021.

sampling site GE3 started to thermally stratify in April when the surface temperature was close to 9 °C. In June, the lake was well stratified with a surface temperature of 18.6 °C and

a thermocline situated at around 13 m. No distinct peak in chlorophyll a could be detected between January and April (Fig. 3) with concentrations around or below  $1 \mu g L^{-1}$  for the two







Fig. 4 Monthly change in the biomass of phytoplankton groups at point G3 from January to November 2021 and corresponding change of  $\text{invAs}_{\text{tot,dis}}$  in the water column. Specific As mass inventories of  $\text{As}_{\text{tot,dis}}$  were calculated by adding concentrations in layers of a virtual column of  $1 \text{ dm}^2$  section area and the height of the corresponding layer. CON: conjugatophyceae, CHL: chlorophyceae, DIA: diatoms; XAN: xantophyceae, CHR: chrysophyceae, CRY: cryptophyceae; DIN: dinophyceae, and CYA: cyanophyceae.

first months of the year. During April sampling, the highest concentrations of chlorophyll a were observed at 14.2 m and they generally decreased with depth. Concentrations decreased sharply between April and May. In June, chlorophyll a concentrations peaked at 9.8 m. This peak was followed by a sharp decline and, similar to May, concentrations approached  $0 \mu\text{g L}^{-1}$  at the bottom of the lake. A monthly change in the biomass of the different phytoplankton groups is shown in Fig. 4. This figure includes data for the whole year 2021. While the water was evenly saturated in oxygen across the depth from January to March, it became oversaturated in April (Fig. 3). In May, surface waters were slightly oversaturated with oxygen and the onset of oxygen depletion could be observed towards the bottom of the lake. This tendency was further pronounced in June, with values reaching 144% oxygen saturation at 5 m and 66% at the bottom of the lake. Dissolved reactive phosphorous (DRP) concentrations in surface waters were highest in February, with concentrations of  $5.5 \mu\text{g L}^{-1}$  at the surface (Fig. 3). In March, a drop in concentrations could be observed with concentrations across the profile approximately constant (around  $2.0 \mu\text{g L}^{-1}$ ). During the following months, DRP concentrations remained below  $3.5 \mu\text{g L}^{-1}$  except for the lowest sampling depth (65 m), where concentrations increased every month, reaching the highest concentration observed across all samples of  $7.8 \mu\text{g L}^{-1}$ .

In the Grand Lac, surface water temperatures were higher in June than in April (Fig. 5). This difference was limited to the surface layer, since below around 30 m, temperature profiles were reasonably similar between April and June. At the bottom of the lake, the water temperature was about  $6^\circ\text{C}$  for both

months. Chlorophyll a concentrations (Fig. 5) were higher in April than in June, with peaks observed at about the same depth ( $\sim 12 \text{ m}$ ). Surface water in June showed the higher oxygen saturation compared to that in April. Profiles of oxygen saturation were relatively similar below 50 m, with a minimum value of less than 30% reached at the bottom of the lake.

**Total ‘dissolved’ arsenic profiles and mass inventories.** Vertical  $\text{As}_{\text{tot,dis}}$  (and  $\text{sumAs}$ ) concentration profiles were measured from January to June in the Petit Lac (Fig. 3 and Tables SI7 and SI8†). In March, concentrations were much lower than in February and April. The effect is clearly shown in Fig. 3. In fact, the concentrations of  $\text{As}_{\text{tot,dis}}$  in March were significantly different from data from all other months (pairwise Wilcoxon test,  $p < 0.01$ ). In the Grand Lac, lower As concentrations were observed in the surface water compared with the deeper water layers (Fig. 5 and Tables SI9 and SI10†). Concentrations increased starting between 100 m and 150 m and showed a considerable similarity between sampling dates. While  $\text{As}_{\text{tot,dis}}$  was reasonably constant across the first 100 m of the water column on 20 April, a drop in concentration could be observed at 15 m on the second sampling date, with a subsequent recovery back to similar concentrations at further depths.

Specific As mass inventories,  $\text{invAs}_{\text{tot,dis}}$ , i.e. the mass of  $\text{As}_{\text{tot,dis}}$  in an ideal water column of  $1 \text{ dm}^2$  section area were calculated by adding the mass of  $\text{As}_{\text{tot,dis}}$  in the different layers resulting from the product of  $\text{As}_{\text{tot,dis}}$  concentrations multiplied by the thickness of the corresponding layer. This parameter provides an indirect estimation of the incorporation of As into the ‘particulate’ phase, essentially phytoplankton, assuming that, at a given time, no sedimentation occurs. The results are shown in Fig. 4 for the Petit Lac where a clear decrease in As in March is observed, well correlated with an increase in algae growth. Specific As mass inventories for 2021 and the previous six years (all As ‘dissolved’ concentrations measured with the same instrument) are shown in Fig. SI3†, showing a high variability among the years. However, a Kruskal–Wallis test showed no seasonality of  $\text{invAs}_{\text{tot,dis}}$  along these years ( $p = 0.092$ ). Specific As mass inventories in the Grand Lac,  $\text{invAs}_{\text{tot,dis}}$ , for the first 70 m gave very similar values to those of the Petit Lac:  $778 \mu\text{g dm}^{-2}$  vs.  $772$  in April and  $764 \mu\text{g dm}^{-2}$  vs.  $754$  in June, respectively.

**Arsenic redox and methylation speciation.** Profiles of all arsenic species are shown in Fig. 6 and 7 for the Petit Lac and the Grand Lac, respectively. The corresponding values are given in Tables SI12, SI13 and SI14.† A detailed description of the profiles for each species at both sampling points can be found in Section SI2†.

**Monthly follow-up in the Petit Lac.** Solute concentration profiles are functions of the physical (mixing and stratification) and biogeochemical (production and degradation) processes taking place. When winter conditions prevailed at the beginning of the lake sampling campaign at GE3, the water column was well mixed and well oxygenated and with very low photo-synthetic activity. As expected, concentration profiles were constant with depth, with a predominant presence of  $\text{iAs}(\text{v})$  ( $820 \text{ ng L}^{-1}$  vs.  $< 25 \text{ ng L}^{-1}$   $\text{iAs}(\text{III})$ ).  $\text{DMA}(\text{III} + \text{V})$  concentrations were slightly above  $10 \text{ ng L}^{-1}$ . This corroborates previous





Fig. 5 Vertical profiles of temperature, percentage of O<sub>2</sub> saturation, chlorophyll a, and total dissolved arsenic, As<sub>tot,dis</sub> in the Grand Lac (point SHL2) in April (blue) and June (orange) 2021.

observations (Table 1) that showed that, contrary to thermodynamic predictions, iAs(III) is present under oxic conditions either because it is very resilient to oxidation, or because of the presence of a source, or both. It is well known that iAs(III) oxidation by oxygen is extremely slow (*e.g.*, only a few percent of As(III) is oxidised within seven days in the presence of air<sup>48</sup>) but As(III) is also subject to photo-oxidation<sup>49</sup> which could result in relatively low As(III) residence times; for instance, 0.7 to 3 days under the conditions of the Pacific Ocean.<sup>10</sup> However, fast photo-oxidation like that observed in boreal lakes<sup>50</sup> requires the presence of high concentrations of specific types of dissolved organic matter – which is not the case in Lake Geneva.<sup>51</sup> Possible sources of iAs(III), and also of methylated species even under winter conditions, could be produced by photosynthetic activity, even if very low, and minor diffusion from sediments.

The Petit Lac was still entirely vertically mixed in March with concentrations of iAs(V) being lower than in January–February (about 650 ng L<sup>-1</sup>) but higher for iAs(III) and DMA(III + V) (65 and 39 ng L<sup>-1</sup>, respectively). Phosphorous concentrations dropped,

and chlorophyll a and phytoplankton biomass increased, all signs of biological activity. Weather conditions were favourable for algal growth because it was unusually warm at the beginning of March 2021 and insolation was above average (<https://www.meteosuisse.admin.ch/home/service-et-publications/publications.html>). A clear drop in sumAs occurred in March. This drop was also observed in As<sub>tot,dis</sub>, supporting that it was not due to an analytical error or artefact. The drop corresponded to a steep decrease in As(V) not compensated by the increase in other dissolved As-containing species. This suggests that, at this sampling date, As(V) had ‘moved’ from the ‘dissolved’ fraction to the ‘particulate’ one but with a very limited release of iAs(III) and DMA(III + V). Algal blooms could, thus, cause drops in As<sub>tot,dis</sub> by incorporation into algae, but these episodes can be easily missed in monthly sampling campaigns. This phenomenon has been observed in laboratory experiments with *Closterium aciculare*.<sup>52</sup> At the current level of knowledge, it is not possible to relate the observed As retention inside algae to specific phytoplankton species in the lake.





Fig. 6 Vertical profiles of As species ( $iAs(V)$ ,  $iAs(III)$ ,  $MA(III + V)$ ,  $MA(III)$ ,  $DMA(III + V)$ , and  $TMAO$ ) concentrations in the Petit Lac (point GE3) from January to June 2021.

Patterns of As biotransformation differ across phytoplankton species<sup>53</sup> with some algal species transforming  $iAs(V)$  efficiently into  $iAs(III)$  with rapid excretion into the culture medium, while

others accumulate  $iAs(V)$  inside their cells or biotransform it into methylated and other organic As species. Those in the lake might belong to both categories.



In April, surface waters started to stratify at both sampling locations GE3 and SHL2 but mixing still occurred. Surface depletion of  $iAs(v)$  continued, and a minimum was observed at GE3 at 7.5 m, but this time a peak in  $iAs(III)$  appeared at the same depth. The first algal spring bloom seems to be dominated by a build-up of  $iAs(III)$ , which agrees with observations in the literature.<sup>22,52</sup> According to Hellweger *et al.* (2003),<sup>9</sup> the build-up of  $iAs(III)$  is typical for non-P-depleted water bodies. The relationship As–P is further discussed below. The decrease in  $invAs_{dis,tot}$  observed in March 2021 quickly recovered in April, further supporting the view that As had been retained inside algae in March. Although it is risky to draw many conclusions from  $invAs_{dis,tot}$  values because they are a measure of both the amount retained in the floating algae at the moment of sampling and of any possible net losses of As by sedimentation of dead-algae and As in inorganic colloidal particles, in this case the quick recovery can safely be attributed to algae retention. It needs to be mentioned that the annual evolution of  $invAs_{dis,tot}$  is very variable (Fig. SI3†) and important biological mechanisms can be missed if sampling is too widely spaced.

$DMA(III + v)$  concentrations doubled from March to April, indicating strong production similar to  $iAs(III)$ , but the two species showed a very different profile. While the  $iAs(III)$  profile was typical of a compound with a source at 7.5 m, the  $DMA(III + v)$  profile was close to vertical. Values observed in surface water at SHL2 of samples taken on the same day showed a similar tendency. This would suggest that water mixing was faster than the point production for  $DMA(III + v)$ . Although mechanisms of methylation by microalgae remain controversial,<sup>14</sup>  $DMA(v)$  is the final excreted product according to the classical Challenger mechanism<sup>54</sup> and in possible alternative mechanisms. The Challenger mechanism includes reduction of  $iAs(v)$  into  $iAs(III)$  and successive oxidative and reductive methylation steps.

At the end of May,  $iAs(v)$  concentrations recovered, and  $iAs(III)$  and  $DMA(III + v)$  concentrations decreased compared with those in April. After the first algal bloom, the lake was in the clear water phase, a moment between the early spring bloom of algae and the second, summer algal bloom.<sup>30</sup> This is an interesting situation where mechanisms at play are mostly decomposition reactions in the absence of an active source. Anderson and Bruland (1991)<sup>16</sup> showed that the degradation rate of  $DMA(v)$  spiked into waters collected before and after the lake's overturn is very different, the rate being much faster under oxic conditions.  $DMA(v)$  degraded into  $iAs(v)$ . Probably, bacterial processes become important but they remain largely unexplored in oxic waters. For instance, Maki *et al.* (2005)<sup>55</sup> showed that the biomass of  $DMA(v)$  decomposing bacteria peaked approximately one month after the peak in chlorophyll *a* in Lake Kahokugata, Japan, but these bacteria, producing  $iAs(v)$ , needed anaerobic, dark conditions.

The origin of  $MA(III + v)$  remains unclear. These species showed different dynamics from  $DMA(III + v)$ .  $MA(III)$  and  $MA(v)$  are intermediate species formed inside algae but not the final products according to Challenger's and other mechanisms.  $MA(III + v)$  in lake waters could be either released directly from some algae or might be a microbial decomposition product of

$DMA(III + v)$  in the water. Microbial  $DMA$  demethylation had been demonstrated in soils, but not in aquatic systems until Giovannoni *et al.* (2019)<sup>56</sup> showed that the most abundant non-photosynthetic plankton in the oceans, SAR11 bacteria, are able to remove the methyl groups from dimethyl arsenate, releasing monomethyl As and  $iAs(v)$  back to the water.  $MA(III)$  has seldom been measured in freshwaters.<sup>20–22</sup>

In June, a new productivity period peaked (Fig. 4).  $iAs(v)$  concentrations in surface water were depleted and high  $DMA(III + v)$  and  $iAs(III)$  concentrations were established again. Observations at sampling site GE3 showed that the  $DMA(III + v)$  concentration was higher in June than in April, whereas  $iAs(III)$  concentrations showed the reverse trend (Fig. 6). This might be related to the molar  $iAs(v):P$  ratio, which was higher in April than in June (and higher in March than in May). Even if many studies have investigated the role of nutrient availability in the production of As species, it is uncertain how phosphate availability influences their production in different algae.<sup>57</sup> Algae take up more phosphate than needed during the early phases of algal blooms (luxury uptake)<sup>9</sup> and, simultaneously, large quantities of  $iAs(v)$  can enter the cells *via* the same pathway. In oceans, it has been postulated that a high  $iAs(v):P$  ratio causes toxic stress on phytoplankton, promoting fast transformation into  $iAs(III)$  and slow methylation.<sup>46</sup> Kuhn and Sigg (1993)<sup>17</sup> proposed this hypothesis in eutrophic Lake Greifen (ratios < 0.001) to explain the absence of methylated species, but high  $DMA(III + v)$  concentrations were observed in Lake Biwa with high  $iAs(v):phosphate$  ratios.<sup>22</sup> The molar  $iAs(v):P$  ratio at GE3 in Lake Geneva ranged between 0.07 and 0.25 during the sampling period. These ratios are far higher than the ratios covered by ocean studies.<sup>46</sup> It is possible that a higher  $iAs(v)$  stress was exerted on algal communities during the first algal bloom in March and April compared with the second bloom in May–June, which could explain the higher concentration of  $DMA(III + v)$  in June in comparison with that in April. It is also possible, however, that differences in algae species present in the first and second blooms explain the observations.

TMAO has seldom been analysed in surface waters. It was included in none of the studies in Table 1. Like  $MA(III + v)$ , TMAO showed a decreasing trend between January and March at sampling site GE3 (Fig. 6). Increases in surface water began in May. In addition to  $MA(v)$  and  $DMA(v)$ ,  $As(III)$  methylation products also include less toxic As species such as TMAO and volatile trimethylarsine (TMA).<sup>58–60</sup> Savage *et al.* (2018)<sup>61</sup> observed that seawater samples spiked with  $DMA(v)$  led to an enhanced production and volatilisation of TMA into the gaseous phase, with TMAO as a probable intermediate in the aqueous phase. A similar process could lead to observed concentrations of TMAO in lakes.<sup>20</sup> Concentrations of TMAO in January were higher than concentrations of  $MA(III + v)$  and  $DMA(III + v)$ . This observation, considered in the context of the evolution of TMAO concentrations along the studied period, points to TMAO being a rather stable compound, resistant to the processes guiding the system back to the dominance of  $iAs(v)$ , and whose main fate would be its transformation into volatile TMA. In addition, note that our analytical method







Fig. 7 Vertical profiles of As species ( $iAs(V)$ ,  $iAs(III)$ ,  $MA(III,V)$ ,  $MA(III)$ ,  $DMA(III,V)$ , and  $TMAO$ ) concentrations in the Grand Lac (point SHL2) in April (blue) and June (orange) 2021.

cannot distinguish dissolved TMA and TMAO. TMAO is ubiquitous in atmospheric particles;<sup>62</sup> a significant source being pesticides in soils.<sup>63</sup>

*As speciation in lake bottom waters: lessons from the Grand Lac.* The observed dynamics of As speciation at the bottom of Lake Geneva were distinct from the photic zone. In 2021,  $iAs(V)$



concentrations at GE3 at 65 m increased once lake stratification was established. Concentrations reached  $936 \text{ ng L}^{-1}$  in June, which represented 94% of sumAs. The results at the lake's deepest point (SHL2) confirmed iAs(v) dominance at sampling depths below the photic zone (Fig. 7). At both sampling dates (April and June), iAs(v) made up more than 95% of sumAs from 100 m towards the bottom of the lake. At 300 m, independent of the sampling date, the iAs(v) concentration reached almost  $2000 \text{ ng L}^{-1}$ , representing 99% of sumAs. The predominance of iAs(v) agrees with what has been described in the literature: iAs(v) is the dominant species below the photic layer<sup>10,64</sup> in oceans and in freshwaters. For instance, iAs(v) was the main species in the hypolimnion in the highly eutrophic Lake Greifen throughout the whole season,<sup>17</sup> and the observed increase in sumAs with depth in both eutrophic and mesotrophic basins of Lake Biwa in summer was attributed to an increase in iAs(v).<sup>22</sup> The predominance of iAs(v) in lake waters far from the productivity zone is in agreement with thermodynamic predictions and strongly supports the biological origin of iAs(III) when present. On the other hand, increasing iAs(v) concentrations with depth is a direct consequence of the lack of entire lake mixing. Winter mixing remained limited to 145 m in 2021, the depth was reached on 2 March 2021.<sup>29</sup>

While methylated species were evenly distributed across the water column in winter months, differences between the surface water and the bottom layer were established as soon as the lake stratified (Fig. 6). Even if all methylated species showed profiles that resulted from a source in the epilimnion, their shape depended on the species considered. For instance, in June DMA(III + V) concentrations quickly approached a steady concentration with depth, whereas MA(III + V) and TMAO approached their minimum values more slowly at both sampling locations (Fig. 6 and 7). It can thus be assumed that methylated species are subject to decomposition at different rates, with rates for DMA(III + V) transformation being higher than for TMAO. It is interesting that DMA(III + V) values did not approach zero but remained around  $15 \text{ ng L}^{-1}$  in the deepest parts of the lake.

### Exchange of arsenic species between sediment porewaters and the water column

Even if the number of samples was low and they reflected the unavoidable heterogeneity of lake sediments, concentration profiles of As species in the three sediment cores sampled at GE3 provide some interesting information. First,  $\text{As}_{\text{tot,dis}}$  concentrations in the supernatant waters of the three cores were similar:  $1.10 \mu\text{g L}^{-1}$  (C1),  $1.14 \mu\text{g L}^{-1}$  (C2), and  $1.38 \mu\text{g L}^{-1}$  (C3) versus  $1.15 \mu\text{g L}^{-1}$  at 65 m depth in July, but they were always higher below the sediment water interface than in the supernatant water (for instance,  $1.98 \mu\text{g L}^{-1}$  (C1),  $5.95 \mu\text{g L}^{-1}$  (C2), and  $9.52 \mu\text{g L}^{-1}$  (C3) at 2 cm depth) which implies a subsequent input of 'dissolved' As from the sediments to the water column. Secondly, this input is fed by iAs(III) and iAs(v) species since both species show higher concentrations in the interstitial waters compared with in the water column. The most probable

source of 'dissolved' As is the release from the decomposition of sedimented algae, although a contribution from the release from settling iron oxyhydroxides cannot be excluded. A detailed discussion of these mechanisms is, however, entirely outside the scope of this study. Thirdly,  $\text{As}_{\text{tot,dis}}$  in porewaters did not show similar profiles in the three sediment cores (Table SI11†), and profiles also differed for most of the As species measured among sediments (Fig. 8, Table SI15†) but some common patterns were observed: MA(III + V) profiles showed no diffusion or a very weak one and DMA(III + V) and TMAO clearly pointed to a net flux from the water column to the sediments, contrary to iAs(v) and iAs(III). This suggests that DMA(III, V) and TMAO are only – or predominantly – formed in algae.

A rough calculation of diffusion fluxes has been attempted by applying Fick's first law. In the steady state, the flux close to the sediment–water interface is equal to the product of the concentration gradient in the sediment pore waters and the diffusion coefficient of the substance considered. The concentration gradients were calculated from points at 1 and 4 cm depth in the sediments. The calculated fluxes are given in Table 4. Diffusion coefficients for  $\text{As}(\text{OH})_3$  and  $\text{HAsO}_4^{2-}$ ,  $11.6 \times 10^{-6} \text{ cm}^2 \text{ s}^{-1}$  and  $7.27 \times 10^{-6} \text{ cm}^2 \text{ s}^{-1}$ , respectively, are from ref. 65. No corrections for porosity or temperature dependence of the diffusion coefficients were considered since our calculations are only intended to provide a rough quantitative estimation. The mass of As in a  $1 \text{ dm}^2$  layer closer to the lake bottom (57.5 to 75 m) decreased from 136 (January) to 117  $\mu\text{g}$  (March), and increased from March to June (150  $\mu\text{g}$  in 98 days, which means 33  $\mu\text{g}$ ). This corresponds to a mean increase of  $3.90 \times 10^{-5} \text{ ng cm}^{-2} \text{ s}^{-1}$ , which is in the same order of magnitude as the estimated diffusion fluxes of iAs using Fick's Law. This confirms that the order of magnitude of the estimated flux values is correct.

### A complementary insight into arsenic in Lake Geneva tributaries and its possible contribution to lake observations

$\text{As}_{\text{tot,dis}}$  concentrations in the main tributaries to Lake Geneva were in the range  $130\text{--}1200 \text{ ng L}^{-1}$  (Tables 2 and 3) which is congruent with concentrations in stream waters in Europe; median value:  $630 \text{ ng L}^{-1}$ .<sup>66</sup> Concentrations in the Rhone River were higher than those in the lake in April but lower than those in June. Concentrations found in other tributaries were generally lower. The high  $\text{As}_{\text{tot,dis}}$  detected in the Rhone River can be the result of catchment area of the Rhone including areas with elevated natural As concentrations.<sup>67</sup> In June, concentrations in all rivers might have been strongly influenced by weather conditions before the sampling date: heavy thunderstorms occurred at the beginning of June (<https://www.meteosuisse.admin.ch/home/service-et-publications/publications.html>), and rivers were highly turbid and coloured brownish when sampled. The differences in  $\text{As}_{\text{tot,dis}}$  between the two sampling dates in the Rhone River can be related to the differences in water discharge:  $73\text{--}75 \text{ m}^3 \text{ s}^{-1}$  in April and  $504\text{--}541 \text{ m}^3 \text{ s}^{-1}$  in June (points marked with arrows in Fig. SI1†) and could be attributed to a dilution effect, but the establishment of a sound concentration-discharge relationship – usually



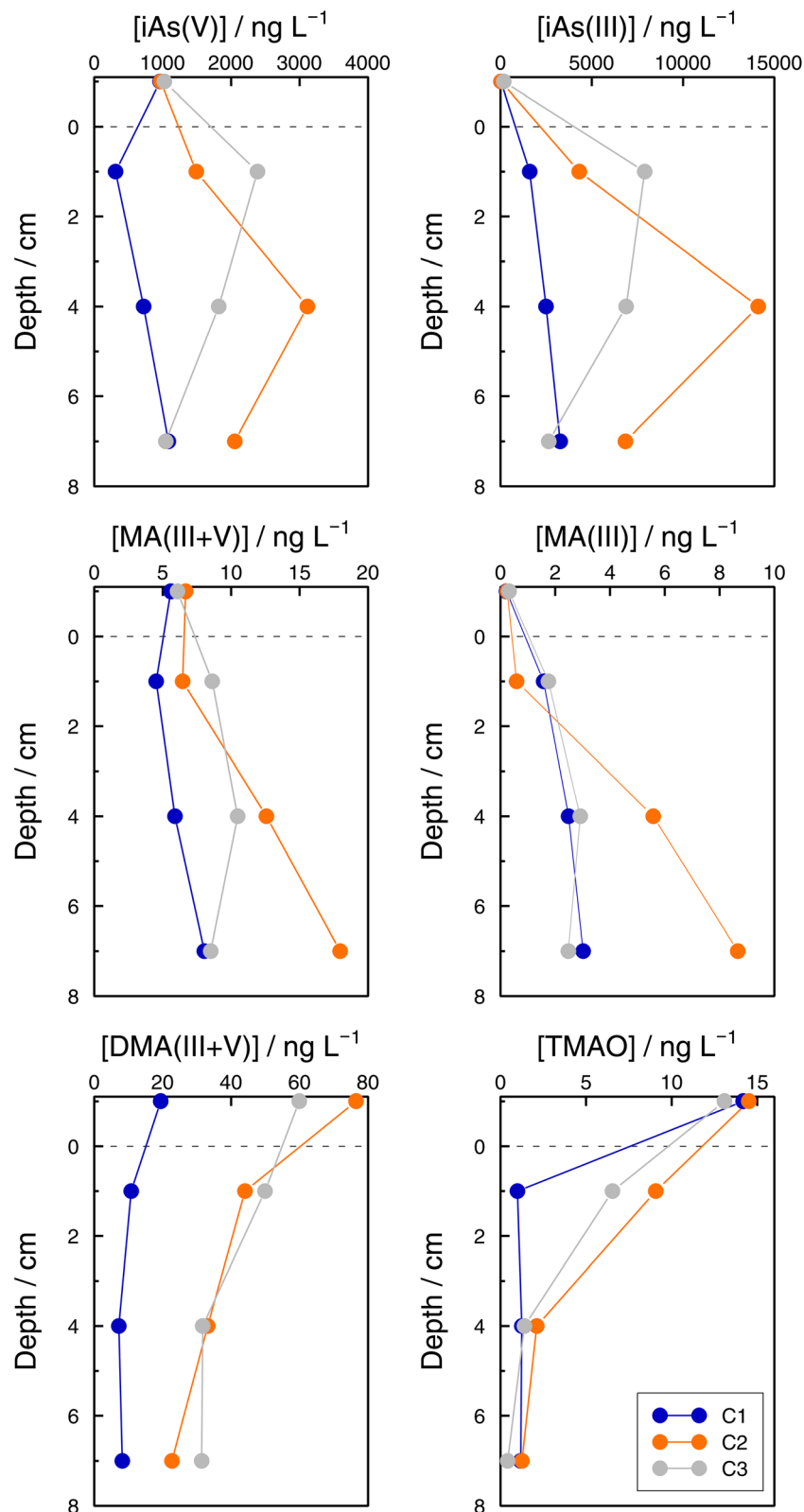


Fig. 8 Concentrations of total dissolved arsenic ( $\text{As}_{\text{tot,dis}}$ ), iAs(v), iAs(III), MA(III + v), DMA(III + v), and TMAO concentrations in sediment pore waters and the overlying supernatant water in three cores (C1 (blue), C2 (orange), and C3 (grey)) in the Petit Lac, 12 July 2021.

following a power law function<sup>68</sup> – would require high frequency discharge data (available) and concentration data (outside current measuring device capabilities) over long periods of

time. Knowledge of such relationships at least for the main tributaries would be essential, for instance, in order to establish a mass balance of the lake.



Core	iAs(III)/ng cm <sup>-2</sup> s <sup>-1</sup>	iAs(V)/ng cm <sup>-2</sup> s <sup>-1</sup>
C1	$-3.46 \times 10^{-6}$	$-9.91 \times 10^{-6}$
C2	$-3.79 \times 10^{-5}$	$-3.93 \times 10^{-6}$
C3	$3.94 \times 10^{-6}$	$1.37 \times 10^{-6}$

Core	iAs(III)/ng cm <sup>-2</sup> s <sup>-1</sup>	iAs(V)/ng cm <sup>-2</sup> s <sup>-1</sup>
C1	$-3.46 \times 10^{-6}$	$-9.91 \times 10^{-6}$
C2	$-3.79 \times 10^{-5}$	$-3.93 \times 10^{-6}$
C3	$3.94 \times 10^{-6}$	$1.37 \times 10^{-6}$



study, the possibility of having access to original analytical data including CRM results has allowed their evaluation, which is somewhat unusual. Adequate quality data tackling allows us to state that ‘dissolved’ As concentrations in Lake Geneva have remained stationary between 1997 and 2021.

(2) State-of-the-art analytical methods are needed in speciation measurements. In particular, great care needs to be taken at the analytical level to ensure the stability of the different species and the absence of measurement artefacts. The steps needed to ensure the preservation of samples are described in detail for application to future studies. Our approach has allowed us to reliably follow the dynamics of  $iAs(v)$ ,  $iAs(III)$ ,  $DMA(III + v)$ ,  $MA(III + v)$  and TMAO in the water column and measure them in river and sediment interstitial waters. We have confirmed the presence of  $MA(III)$  and TMAO in lake and river samples and the predominance of  $iAs(v)$  in most waters.

(3) 'Dissolved' vs. 'particulate' fractions. This study, as with most previous studies, deals with 'dissolved' As, meaning the As that is passed through a filter of a certain pore size. This implies that, if the 'particulate' compartment actively participates in the processes taking place (*e.g.*, through algae in the lake), our interpretation of the results necessarily includes a 'black-box'. This leads to an undesirable degree of speculation when discussing the information obtained.

(4) The role of algae in As speciation in oxic lakes is widely confirmed. Which are the algae involved, as well as the possible role of bacteria in oxic systems remain, however, open questions.

(5) Sampling frequency. In lakes, monthly sampling is not sufficient to adequately follow relevant physical, chemical and biological processes, many of them being much faster. It follows that studies with even lower sampling frequency, as for instance one sampling campaign in summer and one in winter (Table 1), will only be able to provide very limited information.

(6) Inter-year variability. Although, by definition, seasonal variations occur every year, the intensity and temporal location of some processes – particularly biological processes depending on climatic conditions – vary from year to year. This introduces a factor which hinders extrapolation of the results obtained in studies covering only one or a limited number of years. The effects of inter-year variability and modifications linked to climate change need to be considered in future studies.

## Author contributions

M. Filella (conceptualization, data curation, resources, supervision, investigation, project administration, funding acquisition, visualization, validation, writing original draft, writing review and editing); S. Wey (conceptualization, data curation, investigation, visualization, writing original draft, writing review and editing); T. Matoušek (data curation, resources, formal analysis, investigation, validation, methodology, visualization, writing original draft, writing review and editing); M. Coster (resources, validation, funding acquisition, writing review and editing); J.C. Rodriguez-Murillo (data curation, software, formal analysis, validation, writing review and editing); J.-L. Loizeau (resources, supervision, investigation, funding acquisition, validation, writing review and editing).

## Conflicts of interest

There are no conflicts to declare.

## List of abbreviations

AFS	Atomic fluorescence spectrometry
AR(1)	First-order autoregressive process
As <sub>tot,dis</sub>	Total 'dissolved' As concentrations
CON	Conjugatophyceae
CHL	Chlorophyceae
CHR	Chrysophyceae
CRM	Certified reference material
CRY	Cryptophyceae
CT	Cryotrapping
CYA	Cyanophyceae
DIA	Diatoms
DMA(v)	Dimethylarsinate
DIN	Dinophyceae
DMA(III)	Dimethylarsinite
DMA(III + v)	DMA(III) + DMA(v)
DRP	Dissolved reactive phosphorus
EDTA	Ethylenediaminetetraacetic acid
GE3	Sampling point at the Petit Lac (6.2197° E/ 46.2994° N)
HG	Hydride generation
HPLC	High-performance liquid chromatography
iAs	Inorganic As
iAs(III)	Inorganic As(III)
iAs(v)	Inorganic As(v)
ICP-MS	Inductively coupled plasma mass spectrometry
ICP-MS/MS	Inductively coupled plasma–tandem mass spectrometry
invAs <sub>tot,dis</sub>	Specific As mass inventories
MA(III)	Methylarsonite
MA(v)	Methylarsonate
MA(III + v)	MA(III) + MA(v)
MK	Mann–Kendall trend test
REDFIT	Statistical method
SHL2	Sampling point at the Grand Lac (6.5887° E/46.4527° N)
SMK	Seasonal Mann–Kendall trend test
sumAs	Sum of concentrations of all investigated As species
C1	Sediment sampling point, Petit Lac (6.2276° E/46.3052° N)
C2	Sediment sampling point, Petit Lac (6.2201° E/46.2971° N)
C3	Sediment sampling point, Petit Lac (6.2123° E/46.2888° N)
TMA	Trimethylarsine
TMAO	Trimethylarsine oxide
XAN	Xantophyceae
Z	MK statistical parameter

## Acknowledgements

The Institute of Analytical Chemistry of the Czech Academy of Sciences [Institutional support RVO: 68081715] is gratefully acknowledged. We thank Philippe Arpagaus, Vincent Ebener, Emmanuel Farinoli, Jean-Christophe Hustache, Pascal Perney, and Inés Segovia. Without their help, this study would not have been possible.

## References

- 1 J. O. Nriagu, Arsenic poisoning through the ages, in *Environmental Chemistry of Arsenic*, ed. W. T. Frankenberger Jr, Marcel Dekker, Inc., New York, 2002, pp. 1–26.
- 2 R. Nickson, J. McArthur, W. Burgess, K. Matin Ahmed, P. Ravenscroft and M. Rahman, Arsenic poisoning of Bangladesh groundwater, *Nature*, 1998, **395**, 338, DOI: [10.1038/26387](#).
- 3 A. H. Smith, E. O. Lingas and M. Rahman, Contamination of drinking-water by arsenic in Bangladesh: a public health emergency, *Bull. W. H. O.*, 2000, **78**, 1093–1103.
- 4 P. Ravenscroft, H. Brammer and K. Richards, *Arsenic Pollution: a Global Synthesis*, Wiley-Blackwell, Chichester, 2009.
- 5 E. A. Woolson, Fate of arsenicals in different environmental substrates, *Environ. Health Perspect.*, 1977, **19**, 73–81, DOI: [10.1289/ehp.771973](#).
- 6 W. R. Cullen and K. J. Reimer, Arsenic speciation in the environment, *Chem. Rev.*, 1989, **89**, 713–764, DOI: [10.1021/cr00094a002](#).
- 7 R. S. Oremland and J. F. Stolz, The ecology of arsenic, *Science*, 2003, **300**, 939–944, DOI: [10.1126/science.1081903](#).
- 8 S. Silver and L. T. Phung, Genes and enzymes involved in bacterial oxidation and reduction of inorganic arsenic, *Appl. Environ. Microbiol.*, 2005, **71**, 599–608, DOI: [10.1128/AEM.71.2.599-608.2005](#).
- 9 F. Hellweger, K. J. Farley, U. Lall and D. M. Di Toro, Greedy algae reduce arsenate, *Limnol. Oceanogr.*, 2003, **48**, 2275–2288, DOI: [10.4319/lo.2003.48.6.2275](#).
- 10 O. Wurl, R. U. Shelley, W. M. Landing and G. A. Cutter, Biogeochemistry of dissolved arsenic in the temperate to tropical North Atlantic Ocean, *Deep Sea Res., Part II*, 2015, **116**, 240–250, DOI: [10.1016/j.dsr2.2014.11.008](#).
- 11 M. Vahter, Methylation of inorganic arsenic in different mammalian species and population groups, *Sci. Prog.*, 1999, **82**(Pt 1), 69–88, DOI: [10.1177/003685049908200104](#).
- 12 D. J. Thomas, Arsenic methylation - Lessons from three decades of research, *Toxicology*, 2021, **457**, 152800, DOI: [10.1016/j.tox.2021.152800](#).
- 13 K. A. Francesconi and D. Kuehnelt, Determination of arsenic species: A critical review of methods and applications, 2000–2003, *Analyst*, 2004, **129**, 373–395, DOI: [10.1039/B401321M](#).
- 14 Y. Wang, S. Wang, P. Xu, C. Liu, M. Liu, Y. Wang, C. Wang, C. Zhang and Y. Ge, Review of arsenic speciation, toxicity and metabolism in microalgae, *Rev. Environ. Sci. Bio/Technol.*, 2015, **14**, 427–451, DOI: [10.1007/s11157-015-9371-9](#).
- 15 [10.4319/lo.1993.38.5.1052](#).
- 16 A. C. Aurillo, R. P. Mason and H. F. Hemond, Speciation and fate of arsenic in three lakes of the Aberjona watershed, *Environ. Sci. Technol.*, 1994, **28**, 577–585, DOI: [10.1021/es00053a008](#).
- 17 H. M. Spliethoff, R. P. Mason and H. F. Hemond, Interannual variability in the speciation and mobility of arsenic in a dimictic lake, *Environ. Sci. Technol.*, 1995, **29**, 2157–2161, DOI: [10.1021/es00008a041](#).
- 18 D. A. Bright, M. Dodd and K. J. Reimer, Arsenic in subarctic lakes influenced by gold mine effluent: The occurrence of organoarsenicals and “hidden” arsenic, *Sci. Total Environ.*, 1996, **180**, 165–182, DOI: [10.1016/0048-9697\(95\)04940-1](#).
- 19 H. Hasegawa, The behaviour of trivalent and pentavalent methylarsenicals in Lake Biwa, *Appl. Organomet. Chem.*, 1997, **11**, 305–311, DOI: [10.1002/\(SICI\)1099-0739\(199704\)11:4<305::AID-AOC586>3.0.CO;2-6](#).
- 20 Y. Sohrin, M. Matsui, M. Kawashima, M. Hojo and H. Hasegawa, Arsenic biogeochemistry affected by eutrophication in Lake Biwa, Japan, *Environ. Sci. Technol.*, 1997, **31**, 2712–2720, DOI: [10.1021/es960846w](#).
- 21 H. Hasegawa, M. A. Rahman, K. Kitahara, Y. Itaya, T. Maki and K. Ueda, Seasonal changes of arsenic speciation in lake waters in relation to eutrophication, *Sci. Total Environ.*, 2010, **408**, 1684–1690, DOI: [10.1016/j.scitotenv.2009.11.062](#).
- 22 J. L. Barringer, Z. Szabo, T. P. Wilson, J. L. Bonin, T. Kratzer, K. Cenno, T. Romagna, M. Alebus and B. Hirst, Distribution and seasonal dynamics of arsenic in a shallow lake in northwestern New Jersey, USA, *Environ. Geochem. Health*, 2011, **33**, 1–22, DOI: [10.1007/s10653-010-9289-7](#).
- 23 C. Yan, F. Che, L. Zeng, Z. Wang, M. Du, Q. Wei, Z. Wang, D. Wang and Z. Zhen, Spatial and seasonal changes of arsenic species in Lake Taihu in relation to eutrophication, *Sci. Total Environ.*, 2016, **563–564**, 496–505, DOI: [10.1016/j.scitotenv.2016.04.132](#).
- 24 M. J. Palmer, J. Chételat, M. Richardson, H. E. Jamieson and J. M. Galloway, Seasonal variation of arsenic and antimony in surface waters of small subarctic lakes impacted by legacy mining pollution near Yellowknife, NT, Canada, *Sci. Total Environ.*, 2019, **684**, 326–339, DOI: [10.1016/j.scitotenv.2019.05.258](#).
- 25 F. Che, X. Jiang, C. Yao, L. Zhao and K. Wang, Arsenic distribution and speciation in multiphase media of a lake basin, Tibet: The influences of environmental factors on arsenic biogeochemical behavior in the cold arid plateau

- lake, *Sci. Total Environ.*, 2020, **714**, 136772, DOI: [10.1016/j.scitotenv.2020.136772](https://doi.org/10.1016/j.scitotenv.2020.136772).
- 28 S. Ding, Y. Wang, M. Yang, R. Shi, T. Ma, G. Cui and X. Li, Distribution and speciation of arsenic in seasonally stratified reservoirs: Implications for biotransformation mechanisms governing interannual variability, *Sci. Total Environ.*, 2022, **806**, 150925, DOI: [10.1016/j.scitotenv.2021.150925](https://doi.org/10.1016/j.scitotenv.2021.150925).
- 29 CIPEL, *Rapports sur les Études et Recherches Entreprises dans le Bassin Lémanique Campagne 2021*, CIPEL: Nyon, Switzerland, 2022, [www.cipel.org/wp-content/uploads/2022/11/rapport-scientifique-2021-2022-low.pdf](http://www.cipel.org/wp-content/uploads/2022/11/rapport-scientifique-2021-2022-low.pdf), last accessed: 2 January 2023.
- 30 O. Anneville, M. Beniston, N. Gallina, C. Gillet, S. Jacquet, J. Lazzarotto and M. Perroud, L'empreinte du changement climatique sur le Léman, *Arch. Sci.*, 2013, **66**, 157–172, DOI: [10.5169/seals-738482](https://doi.org/10.5169/seals-738482).
- 31 J.-L. Loizeau, S. Makri, P. Arpagaus, B. Ferrari, C. Casado-Martinez, T. Benejam and P. Marchand, Micropolluants métalliques et organiques dans les sédiments superficiels du Léman. Rapport CIPEL contre Pollution, *Campagne*, 2016, **143–198**, 2017.
- 32 T. Matoušek, J. M. Currier, N. Trojánková, J. R. Saunders, M. C. Ishida, C. Gonzalez-Horta, S. Musil, Z. Mester, M. Stýblo and J. Dědina, Selective hydride generation – cryotrapping – ICP-MS for arsenic speciation analysis at picogram levels: analysis of river and sea water reference materials and human bladder epithelial cells, *J. Anal. At. Spectrom.*, 2013, **28**, 1456–1465, DOI: [10.1039/c3ja50021g](https://doi.org/10.1039/c3ja50021g).
- 33 A. García-Figueroa, M. Filella and T. Matoušek, Speciation of germanium in environmental water reference materials by Hydride Generation and Cryotrapping in combination with ICP-MS/MS, *Talanta*, 2021, **225**, 121972, DOI: [10.1016/j.talanta.2020.121972](https://doi.org/10.1016/j.talanta.2020.121972).
- 34 M. Filella and T. Matoušek, Germanium in Lake Geneva (Switzerland/France) along the spring productivity period, *Appl. Geochem.*, 2022, **143**, 105352, DOI: [10.1016/j.apgeochem.2022.105352](https://doi.org/10.1016/j.apgeochem.2022.105352).
- 35 T. Matoušek, A. Hernandez-Zavala, M. Svoboda, L. Langrová, B. M. Adair, Z. Drobná, D. J. Thomas, M. Stýblo and J. Dědina, Oxidation state specific generation of arsines from methylated arsenicals based on L-cysteine treatment in buffered media for speciation analysis by hydride generation-automated cryotrapping-gas chromatography-atomic absorption spectrometry with the multiatomizer, *Spectrochim. Acta, Part B*, 2008, **63**, 396–406, DOI: [10.1016/j.sab.2007.11.037](https://doi.org/10.1016/j.sab.2007.11.037).
- 36 C. Reimann and P. Filzmoser, Normal and lognormal distribution in geochemistry: death of a myth. Consequences for the statistical treatment of geochemical and environmental data, *Environ. Geol.*, 2000, **39**, 1001–1014, DOI: [10.1007/s002549900081](https://doi.org/10.1007/s002549900081).
- 37 R. M. Hirsch and J. R. Slack, A nonparametric trend test for seasonal data with serial dependence, *Water Resour. Res.*, 1984, **20**, 727–732, DOI: [10.1029/WR020i006p00727](https://doi.org/10.1029/WR020i006p00727).
- 38 D. R. Helsel and R. M. Hirsch, *Statistical Methods in Water Resources; Techniques of Water-Resources Investigations of the United States Geological Survey. Book 4*, USGS, Reston, VA, 2002, Ch. A3.
- 39 M. Schulz and M. Mudelsee, REDFIT: estimating red-noise spectra directly from unevenly spaced paleoclimatic time series, *Comput. Geosci.*, 2002, **28**, 421–426, DOI: [10.1016/S0098-3004\(01\)00044-9](https://doi.org/10.1016/S0098-3004(01)00044-9).
- 40 Ø. Hammer, D. A. T. Harper and P. D. Ryan, PAST: Paleontological Statistics Software Package for Education and Data Analysis, *Palaeontol. Electron.*, 2001, **4**, [https://palaeo-electronica.org/2001\\_1/past/issue1\\_01.htm](https://palaeo-electronica.org/2001_1/past/issue1_01.htm).
- 41 J. M. Currier, M. Svoboda, T. Matoušek, J. Dědina and M. Stýblo, Direct analysis and stability of methylated trivalent arsenic metabolites in cells and tissues, *Metallomics*, 2011, **3**, 1347–1354, DOI: [10.1039/c1mt00095k](https://doi.org/10.1039/c1mt00095k).
- 42 D. Yeghicheyan, P. Grinberg, L. Y. Alleman, M. Belhadj, L. Causse, J. Chmeleff, L. Cordier, I. Djouaev, D. Dumoulin, J. Dumont, R. Freydier, H. Mariot, C. Cloquet, P. Kumkrong, B. Malet, C. Jeandel, A. Marquet, J. Riotte, M. Tharaud, G. Billon, G. Trommetter, F. Séby, A. Guihou, P. Deschamps and Z. Mester, Collaborative determination of trace element mass fractions and isotope ratios in AQUA-1 drinking water certified reference material, *Anal. Bioanal. Chem.*, 2021, **413**, 4959–4978, DOI: [10.1007/s00216-021-03456-8](https://doi.org/10.1007/s00216-021-03456-8).
- 43 A. G. Howard and S. D. W. Comber, The discovery of hidden arsenic species in coastal waters, *Appl. Organomet. Chem.*, 1989, **3**, 509–514, DOI: [10.1002/aoc.590030607](https://doi.org/10.1002/aoc.590030607).
- 44 A. M. M. de Bettencourt and M. O. Andreae, Refractory arsenic species in estuarine waters, *Appl. Organomet. Chem.*, 1991, **5**, 111–116, DOI: [10.1002/aoc.590050208](https://doi.org/10.1002/aoc.590050208).
- 45 H. Hasegawa, M. Matsui, S. Okamura, M. Hojo, N. Iwasaki and Y. Sohrin, Arsenic speciation including ‘hidden’ arsenic in natural waters, *Appl. Organomet. Chem.*, 1999, **13**, 113–119, DOI: [10.1002/\(SICI\)1099-0739\(199902\)13:2<113::AID-AOC837>3.0.CO;2-A](https://doi.org/10.1002/(SICI)1099-0739(199902)13:2<113::AID-AOC837>3.0.CO;2-A).
- 46 G. A. Cutter and L. S. Cutter, Biogeochemistry of arsenic and antimony in the North Pacific Ocean, *Geochem., Geophys., Geosyst.*, 2006, **7**, 1–12, DOI: [10.1029/2005GC001159](https://doi.org/10.1029/2005GC001159).
- 47 J.-C. Rodríguez-Murillo, P. Nirel and M. Filella, Detecting trends in freshwater trace element concentrations: methodological issues and data treatment, *H2Open J.*, 2018, **1**, 87–98, DOI: [10.2166/h2oj.2018.006](https://doi.org/10.2166/h2oj.2018.006).
- 48 M. Jekel, Removal of arsenic in drinking water treatment, in *Arsenic in the Environment Part I: Cycling and Characterization*, ed. J. O. Nriagu, Wiley, New York, 1994, pp. 119–132.
- 49 J. Ryu, D. Monllor-Satoca, D. H. Kim, J. Yeo and W. Choi, Photooxidation of arsenite under 254 nm irradiation with a quantum yield higher than unity, *Environ. Sci. Technol.*, 2013, **47**, 9381–9387, DOI: [10.1021/es402011g](https://doi.org/10.1021/es402011g).
- 50 M. Amyot, D. Bélanger, D. F. Simon, J. Chételat, M. Palmer and P. Ariya, Photooxidation of arsenic in pristine and mine-impacted Canadian subarctic freshwater systems, *J. Hazard. Mater. Adv.*, 2021, **2**, 100006, DOI: [10.1016/j.hazadv.2021.100006](https://doi.org/10.1016/j.hazadv.2021.100006).
- 51 J.-C. Rodríguez-Murillo and M. Filella, Temporal evolution of organic carbon concentrations in Swiss lakes: Trends of



- allochthonous and autochthonous organic carbon, *Sci. Total Environ.*, 2015, **520**, 13–22, DOI: [10.1016/j.scitotenv.2015.02.085](#).
- 52 H. Hasegawa, Y. Sohrin, K. Seki, M. Sato, K. Norisuye, K. Naito and M. Matsui, Biosynthesis and release of methylarsenic compounds during the growth of freshwater algae, *Chemosphere*, 2001, **43**, 265–272, DOI: [10.1016/S0045-6535\(00\)00137-5](#).
- 53 H. Hasegawa, R. I. Papry, E. Ikeda, Y. Omori, A. S. Mashio, T. Maki and M. A. Rahman, Freshwater phytoplankton: biotransformation of inorganic arsenic to methylarsenic and organoarsenic, *Sci. Rep.*, 2019, **9**, 1–13, DOI: [10.1038/s41598-019-48477-7](#).
- 54 F. Challenger, Biological methylation, *Chem. Rev.*, 1945, **36**, 315–361, DOI: [10.1021/cr60115a003](#).
- 55 T. Maki, H. Hasegawa and K. Ueda, Seasonal dynamics of dimethylarsinic acid-decomposing bacteria dominating in Lake Kahokugata, *Appl. Organomet. Chem.*, 2005, **19**, 231–238, DOI: [10.1002/aoc.696](#).
- 56 S. J. Giovannoni, K. H. Halsey, J. Saw, O. Muslin, C. P. Suffridge, J. Sun, C.-P. Lee, E. R. Moore, B. Temperton and S. E. Noell, A parasitic arsenic cycle that shuttles energy from phytoplankton to heterotrophic bacterioplankton, *mBio*, 2019, **10**, e00246-19, DOI: [10.1128/mBio.00246-19](#).
- 57 E. G. Duncan, W. A. Maher and S. D. Foster, Contribution of arsenic species in unicellular algae to the cycling of arsenic in marine ecosystems, *Environ. Sci. Technol.*, 2015, **49**, 33–50, DOI: [10.1021/es504074z](#).
- 58 S. Maeda, K. Kusadome, H. Arima, A. Ohki and K. Naka, Biomethylation of arsenic and its excretion by the alga *Chlorella vulgaris*, *Appl. Organomet. Chem.*, 1992, **6**, 407–413, DOI: [10.1002/aoc.590060416](#).
- 59 Suhendrayatna, A. Ohki, T. Kuroiwa and S. Maeda, Arsenic compounds in the freshwater green microalga *Chlorella vulgaris* after exposure to arsenite, *Appl. Organomet. Chem.*, 1999, **13**, 127–133, DOI: [10.1002/\(SICI\)1099-0739\(199902\)13:2<127::AID-AOC810>3.0.CO;2-K](#).
- 60 X. X. Yin, J. Chen, J. Qin, G. X. Sun, B. P. Rosen and Y. G. Zhu, Biotransformation and volatilization of arsenic by three photosynthetic cyanobacteria, *Plant Physiol.*, 2011, **156**, 1631–1638, DOI: [10.1104/pp.111.178947](#).
- 61 L. Savage, M. Carey, P. N. Williams and A. A. Meharg, Biovolatilization of arsenic as arsines from seawater, *Environ. Sci. Technol.*, 2018, **52**, 3968–3974, DOI: [10.1021/acs.est.7b06456](#).
- 62 T. Tziaras, S. A. Pergantis and E. G. Stephanou, Investigating the occurrence and environmental significance of methylated arsenic species in atmospheric particles by overcoming analytical method limitations, *Environ. Sci. Technol.*, 2015, **49**, 11640–11648, DOI: [10.1021/acs.est.5b02328](#).
- 63 H. Mukai and Y. Ambe, Detection of monomethylarsenic compounds originating from pesticide in airborne particulate matter sampled in an agricultural area in Japan, *Atmos. Environ.*, 1987, **21**, 185–189, DOI: [10.1016/0004-6981\(87\)90284-8](#).
- 64 M. O. Andreae, Arsenic speciation in seawater and interstitial waters: The influence of biological-chemical interactions on the chemistry of a trace element, *Limnol. Oceanogr.*, 1979, **24**, 440–452, DOI: [10.4319/lo.1979.24.3.0440](#).
- 65 M. Tanaka, Y. Takahashi, N. Yamaguchi, K.-W. Kim, G. Zheng and M. Sakamitsu, The difference of diffusion coefficients in water for arsenic compounds at various pH and its dominant factors implied by molecular simulations, *Geochim. Cosmochim. Acta*, 2013, **105**, 360–371, DOI: [10.1016/j.gca.2012.12.004](#).
- 66 R. Salminen, M. J. Batista, M. Bidovec, A. Demetriades, B. De Vivo, W. De Vos, M. Duris, A. Gilucis, V. Gregorauskiene, J. Halamic, P. Heitzmann, A. Lima, G. Jordan, G. Klaver, P. Klein, J. Lis, J. Locutura, K. Marsina, A. Mazreku, P. J. O'Connor, S. A. Olsson, R.-T. Ottesen, V. Petersell, J. A. Plant, S. Reeder, I. Salpeteur, H. Sandström, U. Siewers, A. Steenfelt and T. Tarvainen, *Geochemical Atlas of Europe. Part 1: Background Information, Methodology and Maps*, Geological Survey of Finland, Espoo, 2005.
- 67 H.-R. Pfeifer, A. Häussermann, J. C. Lavanchy and W. Halter, Distribution and behavior of arsenic in soils and waters in the vicinity of the former gold-arsenic mine of Salanfe, Western Switzerland, *J. Geochem. Explor.*, 2007, **93**, 121–134, DOI: [10.1016/j.gexplo.2007.01.001](#).
- 68 S. E. Godsey, J. W. Kirchner and D. W. Clow, Concentration–discharge relationships reflect chemostatic characteristics of US catchments, *Hydrol. Processes*, 2009, **23**, 1844–1864, DOI: [10.1002/hyp.7315](#).
- 69 W. Baeyens, A. de Brauwere, N. Brion, M. D. Gieter and M. Leermakers, Arsenic speciation in the River Zenne, Belgium, *Sci. Total Environ.*, 2007, **384**, 409–419, DOI: [10.1016/j.scitotenv.2007.05.044](#).
- 70 R. Bernard, F. Straub, L. Vuataz and M. Balet, *Le Rhône – Observation de la qualité des eaux de surface 2017. Canton du Valais: Département de la mobilité, du territoire et de l'environnement. Service de l'environnement*, Sion, Switzerland, 2018, [www.vs.ch/documents/19415/1603474/Qualit%E9deseauxduRh%F4neenavald%3FEvionnaz%2CCampagne2017/acc4aebc-7ad8-46e3-be60-777eb16fc8ad?t=.now?long](http://www.vs.ch/documents/19415/1603474/Qualit%E9deseauxduRh%F4neenavald%3FEvionnaz%2CCampagne2017/acc4aebc-7ad8-46e3-be60-777eb16fc8ad?t=.now?long), last accessed: 31 December 2022.
- 71 C. M. Casado-Martinez, L. Molano-Leno, D. Grandjean, L. F. De Alencastro, I. Werner and B. J. D. Ferrari, Impact des sédiments sur la qualité de l'eau - Surveillance écotoxicologique de la qualité de la rivière Venoge, *Aqua Gas*, 2016, **4**, 56–63, <https://www.dora.lib4ri.ch/eawag/islandora/object/eawag:10561>.

